Photosynthesis Research (2019) 142:17–34
https://doi.org/10.1007/s11120-019-00643-8

ORIGINAL ARTICLE

Proteomic responses to ocean acidification of the marine diazotroph *Trichodesmium* under iron-replete and iron-limited conditions

Futing Zhang[1] · Haizheng Hong[1,2,3] · Sven A. Kranz[4] · Rong Shen[1] · Wenfang Lin[1] · Dalin Shi[1,2,3]

Received: 15 November 2018 / Accepted: 30 April 2019 / Published online: 10 May 2019

Abstract

Growth and dinitrogen (N_2) fixation of the globally important diazotrophic cyanobacteria *Trichodesmium* are often limited by iron (Fe) availability in surface seawaters. To systematically examine the combined effects of Fe limitation and ocean acidification (OA), *T. erythraeum* strain IMS101 was acclimated to both Fe-replete and Fe-limited concentrations under ambient and acidified conditions. Proteomic analysis showed that OA affected a wider range of proteins under Fe-limited conditions compared to Fe-replete conditions. OA also led to an intensification of Fe deficiency in key cellular processes (e.g., photosystem I and chlorophyll *a* synthesis) in already Fe-limited *T. erythraeum*. This is a result of reallocating Fe from these processes to Fe-rich nitrogenase to compensate for the suppressed N_2 fixation. To alleviate the Fe shortage, the diazotroph adopts a series of Fe-based economic strategies (e.g., upregulating Fe acquisition systems for organically complexed Fe and particulate Fe, replacing ferredoxin by flavodoxin, and using alternative electron flow pathways to produce ATP). This was more pronounced under Fe-limited-OA conditions than under Fe limitation only. Consequently, OA resulted in a further decrease of N_2- and carbon-fixation rates in Fe-limited *T. erythraeum*. In contrast, Fe-replete *T. erythraeum* induced photosystem I (PSI) expression to potentially enhance the PSI cyclic flow for ATP production to meet the higher demand for energy to cope with the stress caused by OA. Our study provides mechanistic insight into the holistic response of the globally important N_2-fixing marine cyanobacteria *Trichodesmium* to acidified and Fe-limited conditions of future oceans.

Keywords Ocean acidification · Photosynthesis · Nitrogen fixation · Diazotrophs · Iron limitation

Introduction

The ubiquitous filamentous cyanobacteria *Trichodesmium* represent one of the potent providers of nitrogen (N) to marine ecosystems, contributing about half of the global oceanic dinitrogen (N_2) fixation (Mahaffey et al. 2005). This diazotroph thus plays a pivotal role in the regulation of the biogeochemical cycles of N and carbon (C) in oligotrophic oceans (Galloway et al. 1995; Gruber and Sarmiento 1997). In addition, *Trichodesmium* is also an important player in the oceanic iron (Fe) cycle, due to its capacities to dissolve and acquire Fe directly from dust deposition at the ocean surface (Rubin et al. 2011; Basu and Shaked 2018). Therefore, it is of critical importance to better understand the response of *Trichodesmium* to changing ocean conditions such as the ongoing ocean acidification (OA), which is caused by the increasing dissolution of anthropogenic carbon dioxide (CO_2) into the oceans (Caldeira and Wickett 2003; Doney et al. 2009).

Futing Zhang and Haizheng Hong have contributed equally to this work.

Electronic supplementary material The online version of this article (https://doi.org/10.1007/s11120-019-00643-8) contains supplementary material, which is available to authorized users.

✉ Dalin Shi
dshi@xmu.edu.cn

[1] State Key Laboratory of Marine Environmental Science, Xiamen University, Xiamen, Fujian, People's Republic of China

[2] Fujian Provincial Key Laboratory for Coastal Ecology and Environmental Studies, Xiamen University, Xiamen, Fujian, People's Republic of China

[3] College of the Environment and Ecology, Xiamen University, Xiamen, Fujian, People's Republic of China

[4] Department of Earth, Ocean and Atmospheric Science, Florida State University, Tallahassee, FL 32306, USA

However, the effects of OA on *Trichodesmium* are complex. Several studies have shown that OA stimulated N_2 fixation and growth of *Trichodesmium* under nutrient-replete conditions (e.g., Hutchins et al. 2007; Levitan et al. 2007; Kranz et al. 2010; Walworth et al. 2016). Such beneficial effects of OA have been attributed to the downregulation of the CO_2-concentrating mechanisms (CCMs) by the increasing partial pressure of CO_2 (pCO_2) in seawater which presumably saves energetic resources for both growth and N_2 fixation (Kranz et al. 2011). However, no significant changes in the proteome of nutrient-replete *Trichodesmium* have been found in response to elevated pCO_2, which would have supported the observed growth stimulation (Walworth et al. 2016). In contrast, recent laboratory and field studies have reported no significant or even negative effects of OA on *Trichodesmium* (Shi et al. 2012; Böttjer et al. 2014; Gradoville et al. 2014; Eichner et al. 2014; Hong et al. 2017). These contradictory findings could have been due to the different culture media used by different studies. As suggested by Shi et al. (2017), contamination and poor trace-metal buffering (afforded by the low EDTA concentration) in artificial seawater media, which cause suboptimal growth rates of *Trichodesmium*, are likely responsible for the reported beneficial effects of OA. In well-defined "clean" natural seawater-based media that promote fast growth rates, however, *Trichodesmium* responds either negligibly or even negatively to OA (Hong et al. 2017; Shi et al. 2017). More recently, an optimality-based cellular model study quantitatively analyzed the allocation of cellular energy among key cellular processes in response to OA (Luo et al. 2019). The results indicated that the energetic benefit of a CCM downregulation by increasing pCO_2 for *Trichodesmium* is limited, and hence, it is unlikely to support a previously observed substantial increase in growth and N_2-fixation rates under OA (Luo et al. 2019). Furthermore, by separating the effects of pH decrease from those of the concomitant increase in pCO_2, Hong et al. (2017) showed that low seawater pH negatively affected *Trichodesmium*, since it reduced cytosolic pH and nitrogenase efficiency, thus demanding additional energy and resources to cope with the adverse effects. Overall, these previous studies suggested that the net response of *Trichodesmium* to OA depends largely on both the energy and resource availability and their allocation to cellular processes to balance cellular demands.

In marine phytoplankton, Fe plays an essential role for various key biochemical processes such as energy metabolism, removal of reactive oxygen species (ROS), and nutrient assimilation. Cyanobacteria generally have a higher Fe requirement than other phytoplankton groups (Brand 1991). As diazotrophic cyanobacteria, *Trichodesmium* have a further enhanced Fe demand mainly due to their Fe-rich nitrogenase, the enzyme that catalyzes N_2 fixation (Kustka et al. 2003). Hence, the growth of *Trichodesmium* is often limited by low Fe availability in surface waters of tropical and subtropical oligotrophic oceans where they thrive (Sohm et al. 2011; Snow et al. 2015a). Apart from nitrogenase, *Trichodesmium* invests a significant portion of its intracellular Fe in photosystems, especially under Fe-limited conditions (Kustka et al. 2003; Snow et al. 2015b). It has been suggested that the ongoing acidification of seawater will likely decrease the bioavailability of dissolved Fe to marine phytoplankton (Shi et al. 2010). Thus, it is imperative to mechanistically elucidate the combined effects of OA and Fe limitation on the globally important N_2-fixing marine cyanobacteria *Trichodesmium* in order to predict the ecological and biogeochemical significance of this organism in a future ocean.

The responses of protein expression to Fe limitation in *Trichodesmium* include the reduction in the Fe-rich nitrogenase, the reduced Fe-containing photosynthetic proteins and photosystem I (PSI):photosystem II (PSII) ratio, and an induction of the Fe-stress biomarker FutA/IdiA (ferric uptake transporter A/iron deficiency-induced A) (Shi et al. 2007, 2012; Snow et al. 2015b). In addition, Snow et al. (2015b) suggested a stronger reliance on alternate photosynthetic pathways and an increase in the abundance of proteins that are involved in Fe uptake in *Trichodesmium* under Fe limitation. Walworth et al. (2016) also reported significant induction of the Fe-stress biomarker IdiA, yet nitrogenase expression was not decreased under Fe-limited conditions, which contradicts the findings of many other studies (e.g., Shi et al. 2007, 2012; Richier et al. 2012; Snow et al. 2015b).

It is thought that the response of *Trichodesmium* to OA largely depends on energy and resource availability (in particular Fe), and it has been shown that Fe deficiency can modulate the effects of OA on *Trichodesmium*. For instance, in Fe-limited *Trichodesmium*, the loss of N_2-fixation efficiency due to low pH and the compensative increase of nitrogenase expression under OA have been observed, alongside decreases in the abundance of Fe-containing proteins involved in photosynthesis and respiration (Shi et al. 2012; Hong et al. 2017). Consequently, OA led to a more significant decrease in both growth and N_2-fixation rates in Fe-limited *Trichodesmium* than in Fe-replete cells (Shi et al. 2012; Hong et al. 2017). Walworth et al. (2016) recently reported a decreased nitrogenase expression under OA in Fe-limited *Trichodesmium*. However, this was not reflected in growth rates, and their study did not report N_2-fixation rates. These results are different from those of Hong et al. (2017), which could have been caused by the utilized culture media that support suboptimal growth rates (Shi et al. 2017), and/or by the way (or the duration of) Fe limitation is enforced in Walworth et al. (2016). Therefore, in addition to the above-mentioned changes in N_2 fixation, photosynthesis, and respiration, the holistic responses to OA of metabolic

processes (including those involved in Fe acquisition and utilization) in Fe-limited *Trichodesmium* remain to be fully understood.

In this study, *T. erythraeum* strain IMS101 (hereafter *T. erythraeum*) was acclimated for 3 months to both replete and limiting concentrations of Fe under both ambient (400 µatm CO_2, pH 8.02) and acidified (740 µatm CO_2, pH 7.81) conditions. The utilized natural seawater medium (Aquil-tricho) was prepared using surface water that was collected from the oligotrophic South China Sea. This medium has a well-defined chemistry that supports optimal growth of *Trichodesmium* (Shi et al. 2017). The effects of OA on the key Fe-related biological processes were systematically examined by semiquantitative proteomics using iTRAQ LC–ESI–MS/MS techniques. The findings of this study shed new light on the response of this widespread marine diazotroph to OA under Fe-limited conditions.

Materials and methods

Culturing and experimental design

The marine cyanobacterium *T. erythraeum* strain IMS101 was obtained from the National Center for Marine Algae and Microbiota (Maine, USA). Culturing was conducted in Aquil-tricho medium prepared with 0.22 µm filtered and microwave-sterilized oligotrophic surface water of the South China Sea (Hong et al. 2017). Trace-metal clean techniques were applied for seawater sampling, the preparation of culture medium, and both culturing and experimental manipulations. The background concentration of dissolved Fe in the collected natural seawater was estimated to be 0.2 nM (Wen et al. 2006; Jiann and Wen 2012). The growth medium was enriched with 10 µM chelexed and filter-sterilized NaH_2PO_4, filter-sterilized vitamins and trace metals (8 nM Cu, 20 nM Zn, 8 nM Co, 20 nM Ni, 10 nM Se, and 18 nM Mn) buffered with 20 µM EDTA (Sunda et al. 2005; Hong et al. 2017), and various concentrations of total dissolved Fe (Fe_T). Cultures were unialgal and grown at 27 °C and 80 µmol photons m^{-2} s^{-1} (14 h : 10 h light–dark cycle) in an AL-41L4 algae chamber (Percival). Although cultures were not axenic, sterile techniques were applied for culturing and experimental manipulations.

Experimental cultures of *T. erythraeum* were acclimated to experimental conditions for about 3 months at two Fe levels (Fe-limited and Fe-replete) under both ambient (400 µatm CO_2, pH 8.02) and acidified (740 µatm CO_2, pH 7.81) conditions. The carbonate chemistry of the growth medium was manipulated via bubbling with humidified and 0.22 µm filtered CO_2–air mixtures that were generated by CO_2 mixers (Ruihua Instrument & Equipment Ltd, China). The pH_T (pH on the total scale) of media was monitored daily throughout the experimental period using a spectrophotometric method (Zhang and Byrne 1996), and drifted by <0.1 units by the end of each dilution cycle. The dissolved inorganic carbon (DIC) concentration was analyzed by acidification and subsequent quantitation of released CO_2 with a CO_2 analyzer (LI 7000, Apollo SciTech, USA). Calculations of alkalinity and pCO_2 were made using the CO2Sys program (Pierrot et al. 2006) based on measurements of pH_T and DIC using the carbonic acid dissociation constants of Mehrbach et al. (1973) that were refit in different functional forms by Dickson and Millero (1987). Carbonate chemistry of the different experimental treatments is shown in Table S1. Based on light, temperature, EDTA concentration (20 µM), and pH of the media, to maintain constant bioavailable Fe concentrations (Fe') at 35 pM for Fe-limited treatments, the added Fe_T (including the estimated 0.2 nM background Fe) were 10.5 and 32.5 nM (calculated following Sunda et al. 2005) in ambient and acidified cultures, respectively. For Fe-replete treatments, the constant Fe' was 925 pM, and thus the Fe_T were 300.5 and 765.5 nM in ambient and acidified cultures, respectively.

During acclimation, the chlorophyll *a* (Chl *a*) concentration and cell abundance were measured at least four times during the exponential phase of one dilution cycle (at days 1, 2, 3, and 4 of the Fe-replete treatments and at days 1, 3, 5, and 7 of the Fe-limited treatments), and the sampling time was consistently in the middle of the photoperiod. Cell-specific growth rates (µ) were determined via linear regressions of the natural logarithm of cell density versus time. The growth rates of each treatment reached steady-state after one-month of acclimation and remained stable for two more months before harvesting in mid-exponential phase for measurement of elemental composition, Western blotting, and both C- and N_2-fixation rates. The experiments were carried out in triplicates, and the representative growth rates of the last dilution cycle were reported. Samples for proteomic analysis were obtained from a separate experiment where *T. erythraeum* had been cultured under the same experimental conditions and was collected in the same manner as in the present study (Hong et al. 2017).

Chl *a* concentration and cell abundance

To measure Chl *a*, *T. erythraeum* was filtered onto 3-µm polycarbonate membrane filters (Millipore). Chl *a* was extracted by heating the filter at 70 °C for 6 min in 90% (vol/vol) methanol. The filter was then removed and centrifuged at 14,000 rpm for 5 min. The absorbances of the supernatant were measured at 665 and 750 nm using a spectrophotometer and was calculated based on Tandeau De Marsac and Houmard (1988). Cell abundance was determined using an inverted microscope, equipped with a Sedgwick-Rafter counting chamber. For each culture, the total length and

cell numbers of about 20 filaments were first measured to determine the average cell length. Cell density was then determined by dividing the total length of filaments in 2 mL culture by the average cell length. In addition, the cell width was also measured as a further proxy for cell size in addition to cell length. The average cell size (cell length and width) is shown in Fig. S1.

Elemental composition

To determine both particulate organic carbon (POC) and nitrogen (PON), samples were collected on pre-combusted 25-mm-diameter glass fiber (GF/F) filters and stored at − 80 °C. Prior to analysis, the filters were dried in an oven overnight at 60 °C, fumed with HCl for 6 h to remove all inorganic carbon, and again dried overnight at 60 °C. After packing into tin cups, POC and PON in the filters were measured with a PerkinElmer 2400 Series II CHNS/O elemental analyzer (USA).

C- and N_2-fixation rates

Short-term C-uptake rates were determined by adding 10 µCi $NaH^{14}CO_3$ (PerkinElmer, USA) to 50 mL of exponentially growing cultures at 0, 1, 3, 5, 7, 9, 11, and 13 h after light onset and incubated under the growth conditions described above for 20 min. After incubation, the samples were collected via filtration onto 3-µm polycarbonate membrane filters (Millipore, Massachusetts, USA), washed with 0.22 µm filtered oligotrophic seawater, and placed at the bottom of scintillation vials. The filters were acidified to remove inorganic C by adding 500 µL of 2% HCl and allowing overnight incubation, after which the samples were heated to dry to remove HCl. The radioactivity was determined using a liquid scintillation analyzer (Tri-Carb 2800TR, PerkinElmer, USA).

The N_2-fixation rate was determined at the midpoint of the light period via acetylene reduction assay (ARA) (Capone 1993). Although this may overlook part of the N_2 fixation occurring toward the end of the light period (Kranz et al. 2010), previous studies have demonstrated that this method can quantitatively identify N_2-fixation rate changes under different environmental conditions (Berman-Frank et al. 2007; Hong et al. 2017). The samples (15 mL each) were sealed in acid-washed 60-mL serum bottles, injected with acetylene (10% of headspace volume), and incubated for 2 h under the same light and temperature conditions as the original culture. The rate of ethylene production was measured using a gas chromatograph (Shimadzu GC-8A, Shimadzu, Kyoto, Japan), equipped with a flame ionization detector and quantified relative to an ethylene standard. The rates were normalized per cell at a reduction ratio of 4:1 for the conversion of ethylene production to N_2-fixation rates. It should be noted that this ratio can also be lower in *T. erythraeum* grown under ambient conditions compared to grown under acidified conditions (Hong et al. 2017). Thus, the actual N_2-fixation rates under ambient conditions may be underestimated in comparison to under acidified conditions.

Western blotting

Trichodesmium erythraeum cells were collected on 3-µm polycarbonate membrane filters (Millipore), flash frozen in liquid nitrogen, and stored at − 80 °C until extraction. Proteins were extracted and denatured in an extraction buffer (50 mM Tris–HCl pH 6.8, 2% w/v SDS, 10% v/v glycerol, and 1% v/v β-mercaptoethanol) under heating at 100 °C for 10 min, followed by centrifugation at 20,000 g for 5 min to remove insoluble material. Total protein in the supernatant was measured using the bicinchoninic acid (BCA) assay (Thermo Fisher Scientific, California, USA) and equal concentrations of proteins were resolved via SDS-PAGE. The transfer and immunodetection were conducted using primary antibodies from Agrisera (PsaC: Art no. AS10 939; PsbA, Art no. AS05 084) as previously described (Shi et al. 2012).

Protein preparation and digestion

In the middle of the photoperiod, *T. erythraeum* cells, growing at a steady state, were collected by filtration, flash frozen in liquid nitrogen, and stored at − 80 °C until further analysis. Proteins were extracted using lysis buffer (7 M urea, 2 M thiourea, 4% 3-((3-Cholamidopropyl) dimethylammonio)-1-propanesulfonate), 20 mMtris-HCl (CHAPS), pH 8.4) containing 1 mM phenylmethanesulfonyl fluoride (PMSF). After 5 min of vortex, 2 mM EDTA and 10 mM dithiothreitol (DTT) were added to the samples, sonicated on ice, and centrifuged at 17,000×*g* for 30 min at 4 °C. The supernatant was mixed with ice-cold acetone (1:5, v/v) containing 20 mM DTT, and the mixture was incubated at − 20 °C overnight. After centrifugation at 17,000×*g* for 30 min at 4 °C, the precipitate was collected, washed twice with ice-cold acetone containing 20 mM DTT, and air-dried. To reduce disulfide bonds, the dry samples were re-dissolved in lysis buffer containing 10 mM DTT and incubated at 56 °C for 1 h. Subsequently, 55 mM iodoacetamide (IAM) was added to the samples and incubated for a further 1 h in the dark to block cysteine residues. The samples were precipitated with ice-cold acetone, air-dried, and finally dissolved in 0.5 M tetraethyl ammonium bromide (TEAB; Applied Biosystems, Milan, Italy). Protein (100 µg each) was digested with Trypsin Gold (Promega, Madison, WI, USA) (30:1,

protein:trypsin) at 37 °C for 16 h and dried via vacuum centrifugation.

iTRAQ Labeling and SCX fractionation

Peptides were reconstituted in 0.5 M TEAB buffer and processed according to the manufacturer's protocol for 4-plex iTRAQ reagent labeling (Applied Biosystems). After incubation at room temperature for 2 h, the labeled peptide mixtures were pooled and dried via vacuum centrifugation. SCX chromatography was performed with a LC-20AB HPLC pump system (Shimadzu, Kyoto, Japan). iTRAQ-labeled peptide mixtures were reconstituted in 4 mL buffer A (25 mM NaH_2PO_4 in 25% acetonitrile, pH 2.7) and loaded onto a 4.6 × 250 mm Ultremex SCX column containing 5 µm particles (Phenomenex, California, USA). The peptides were eluted at a flow rate of 1 mL/min with a gradient of buffer A for 10 min, 5–60% buffer B (25 mM NaH_2PO_4, 1 M KCl in 25% acetonitrile, pH 2.7) for 27 min, and 60–100% buffer B for 1 min. The elution was monitored by measuring the absorbance at 214 nm and the eluted peptides were pooled into 20 fractions, desalted with a Strata-X C18 column (Phenomenex), vacuum-dried, and resuspended in buffer C (2% acetonitrile and 0.1% formic acid).

LC–ESI–MS/MS analysis

Peptides were separated using a LC-20AD nano HPLC (Shimadzu, Kyoto, Japan). Peptides were loaded onto a 10 cm analytical C18 column packed in-house at 8 µL min^{-1} for 4 min and eluted at a flow rate of 300 nL min^{-1}. Buffer C was used as initial buffer and the elution gradient was 44 min 0-35% buffer D (98% ACN and 0.1% FA) followed by 2 min linear gradient to 80% buffer D, maintenance at 80% buffer D for 4 min, and finally returning to 100% buffer C in 1 min.

The eluate was subjected to nanoelectrospray ionization followed by tandem mass spectrometry in an Orbitrap mass spectrometer (Q Exactive, Thermo Fisher Scientific, California, USA). Intact peptides were detected with a resolution of 70,000 and were selected for MS/MS using the higher-energy collision dissociation (HCD) operating mode at a normalized collision energy setting of 27. Ion fragments were detected in the Orbitrap at a resolution of 17,500. A data-dependent procedure was applied for the 15 most abundant precursor ions above a threshold ion count of 20,000 in the MS survey scan.

Bioinformatics analysis

Proteins were identified using the Mascot search engine (version 2.3.02; Matrix Science, London, UK) against the *T. erythraeum* IMS101 database (NCBInr, http://www.ncbi.nlm.nih.gov/Taxonomy/Browser/wwwtax.cgi?id=203124, after removal of redundant sequences). Database search parameters were set as follows: monoisotopic mass; peptide mass tolerance at 20 ppm and fragment mass tolerance at 0.05 Da; trypsin as enzyme; allowing one missed cleavage; +2 and +3 as the peptide; Gln->pyro-Glu (Q) @N-term, oxidation (M), deamidated (NQ) as potential variable modifications; and carbamidomethyl (C), iTRAQ 8-plex (N-term), iTRAQ 8-plex (K) as fixed modifications.

Peptides at 95% confidence interval were counted and filtered at a FDR of 1%, and each protein was identified with at least one unique peptide. For quantitation, a given protein should contain at least two unique peptide spectra. Quantitative protein ratios were weighted and normalized using the median ratio in Mascot. Differentially expressed proteins were analyzed via *t* test and the results were filtered using the Benjamini–Hochberg procedure for FDR correction (5% FDR; Hochberg 1995). Fold changes ≥ 1.2 or ≤ 0.83 were considered significant. Functional annotation of proteins was performed using the Blast2GO software against the non-redundant protein database (NCBInr). The KEGG database (http://www.genome.jp/kegg/) and the COG database (http://www.ncbi.nlm.nih.gov/COG/) were used to classify and group identified proteins.

Statistical analysis

Data were analyzed using SigmaPlot 12.5 (Systat Software, Inc) to determine the statistical significance of differences via one-way analysis of variance (ANOVA) combined with Fisher LSD test. Significant differences in parameters among treatments were indicated using different superscript letters and a significance level of $p < 0.05$ was applied.

Results

Growth, C- and N_2-fixation rates, and elemental compositions

Trichodesmium erythraeum grown under Fe-replete conditions had a considerably higher cell-specific growth rate, N_2-fixation rate, integrated daily C-fixation rate, and POC compared to cells grown under Fe-limited conditions (Fig. 1 and Table 1). OA decreased the growth rates of both Fe-limited and Fe-replete *T. erythraeum* by 23% and 9%, respectively (Fig. 1a, $p < 0.05$). In response to OA, the N_2-fixation rates were suppressed by 57% and 13% under Fe-limited and Fe-replete conditions, respectively (Fig. 1b, $p < 0.05$). The integrated daily C-fixation rate decreased by 53% in

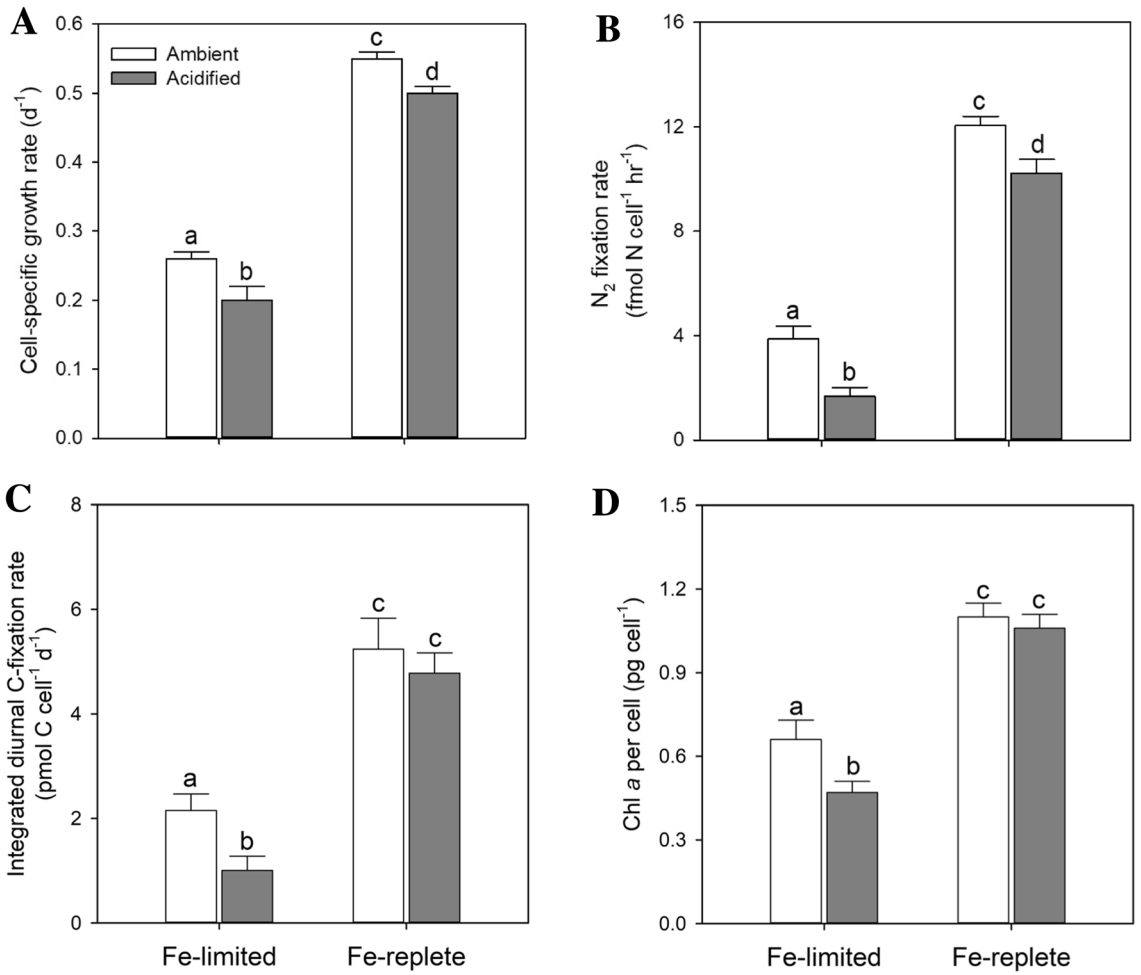

Fig. 1 Effects of OA on **a** the cell-specific growth rate (day^{-1}), **b** the N_2-fixation rate (fmol N cell^{-1} h^{-1}), **c** the integrated diurnal C-fixation rate (pmol C cell^{-1} h^{-1}), and **d** the cellular Chl *a* content (pg cell^{-1}) of *T. erythraeum* strain IMS101 cultured at limiting (35 pM Fe') and replete (925 pM Fe') Fe concentrations under both ambient (400 µatm CO_2, pH 8.02) and acidified (740 µatm CO_2, pH 7.81) conditions. Error bars represent the SD of biological replicates ($n=3$). Different superscript letters indicate significant differences ($p<0.05$) among treatments (one-way ANOVA followed by Fisher LSD test). The growth curves that supplied the growth rates are shown in Fig. S2. C-fixation rates were measured at 0, 1, 3, 5, 7, 9, 11, and 13 h after the onset of light (Fig. S3). Chl *a* per cell was the average of four measurements during the exponential growth phase as shown in Fig. S4

Table 1 POC, PON, and C:N ratios of *T. erythraeum* strain IMS101 cultured at limiting (35 pM Fe') and replete (925 pM Fe') Fe concentrations under both ambient (400 µatm CO_2, pH 8.02) and acidified (740 µatm CO_2, pH 7.81) conditions

Treatments	POC (pmol C cell^{-1})	PON (pmol N cell^{-1})	POC:PON (mol/mol)
Fe-limited			
Ambient	4.30 ± 0.26^{a}	0.49 ± 0.03^{a}	8.72 ± 0.74^{a}
Acidified	3.67 ± 0.08^{b}	0.42 ± 0.04^{b}	8.69 ± 0.79^{a}
Fe-replete			
Ambient	6.63 ± 0.52^{c}	1.04 ± 0.08^{c}	6.41 ± 0.09^{b}
Acidified	6.89 ± 0.55^{c}	1.08 ± 0.08^{c}	6.35 ± 0.06^{b}

Data represent mean ± SD ($n=3$). Different superscript letters indicate significant differences ($p<0.05$) among treatments (one-way ANOVA followed by Fisher LSD test)

Fe-limited *T. erythraeum* grown under acidified conditions ($p<0.05$); however, it was not significantly affected by OA in Fe-replete cells (Fig. 1c). Cellular POC and PON decreased significantly under Fe limitation ($p<0.05$), and decreased slightly under acidified conditions in the Fe-limited cells (Table 1). Due to the non-Redfield change,

POC/PON ratios increased under Fe limitation; however, no significant difference was found between the different CO_2 concentrations.

Chlorophyll *a* content

The Chl *a* content per cell remained constant during the exponential growth phase for all four treatments (Fig. S4). The average Chl *a* per cell over the growth period was calculated and the results showed that the cellular Chl *a* content of *T. erythraeum* was significantly lower at low Fe concentrations compared to that at high Fe concentrations (Fig. 1d, $p < 0.05$). Under Fe-limited conditions, cultures grown under acidified conditions exhibited a significantly lower cellular Chl *a* (by 29%, $p < 0.05$) compared to those grown under ambient conditions. Acidification, however, had no noticeable influence on the cellular Chl *a* content in Fe-replete *T. erythraeum* (Fig. 1d).

Effects of CO_2 and Fe on the *Trichodesmium erythraeum* proteome

To investigate the responses of *T. erythraeum* to different Fe and CO_2 concentrations, total protein was extracted and analyzed using iTRAQ-LC–MS/MS techniques. A total of 328,559 spectra were acquired, 80,356 of which were unique peptide spectra that matched 10,636 unique peptides. To decrease the probability of false peptide identification, only peptides at the 95% confidence interval were counted and filtered at 1% false discovery rate (FDR). The identified unique peptides belonged to 2360 proteins, and each protein was identified by at least one unique peptide. These identified proteins covered 52% of the 4549 predicted protein-coding genes in the genome of *T. erythraeum* strain IMS101 (www.jgi.doe.gov).

The differentially expressed proteins were identified according to *t*-test. The proteins were filtered using the Benjamini–Hochberg procedure for the FDR correction (5% FDR) and fold changes ≥ 1.2 or ≤ 0.83 were considered significant. A Venn diagram shows the number of differentially expressed proteins in response to different Fe concentrations and acidification under both Fe-limited and Fe-replete conditions (Fig. 2 and Fig. S5). In total, 287 proteins were differentially expressed (182 were upregulated and 105 were downregulated) when the Fe concentration varied (Fe-limited vs. Fe-replete). 184 (96 upregulated and 88 downregulated) and 59 (41 upregulated and 18 downregulated) proteins were differentially expressed in response to OA in Fe-limited and Fe-replete *T. erythraeum*, respectively. This suggests that acidification affects more proteins and metabolic processes under Fe-limited conditions than under Fe-replete conditions. In addition, only seven (six upregulated and one downregulated) out of 4549 proteins were affected by OA in both Fe-limited and Fe-replete *T. erythraeum*, indicating that the metabolic response of the diazotroph is differently regulated by OA under different Fe conditions. It should be noted that temporal segregation of N_2 fixation and photosynthesis has been reported within the photoperiod in *Trichodesmium* (Berman-Frank et al. 2001). The current proteomic analysis to describe the response to the experimental treatments (i.e., Fe and pCO_2/pH) was conducted with samples collected in the middle of the photoperiod, and thus, the observed changes in the proteome correspond to the time point at which Fe requirement for N_2 fixation is supposed to be the highest. Diel changes in protein abundance have been shown in Snow et al. (2015b), and data shown here may be

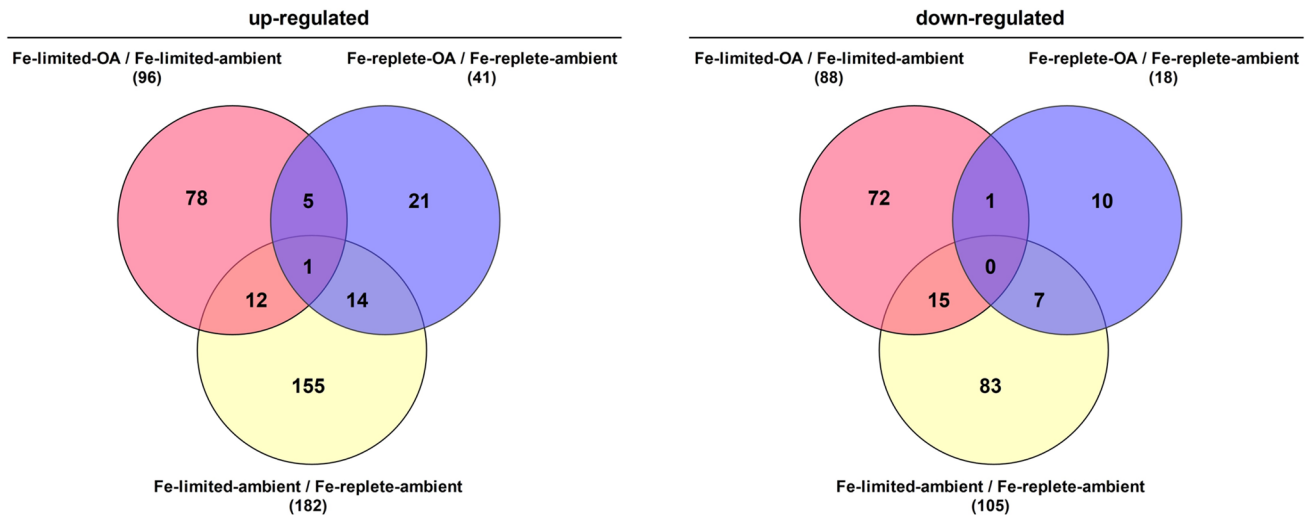

Fig. 2 Venn diagrams denoting the numbers of differentially expressed proteins in *T. erythraeum* strain IMS101 cultured at limiting (35 pM Fe') and replete (925 pM Fe') Fe concentrations under both ambient (400 µatm CO_2, pH 8.02) and acidified (740 µatm CO_2, pH 7.81) conditions

biased against the diurnal cycles of *T. erythraeum.* Yet the focus of this study is to describe the Fe- and/or CO_2-stress responses and not a diurnal regulation in proteins.

Changes in the expressions of Fe-containing and related proteins

To cope with Fe stress, a variety of Fe-containing proteins involved in major biological processes that have high demand for Fe, such as photosynthetic electron transport,

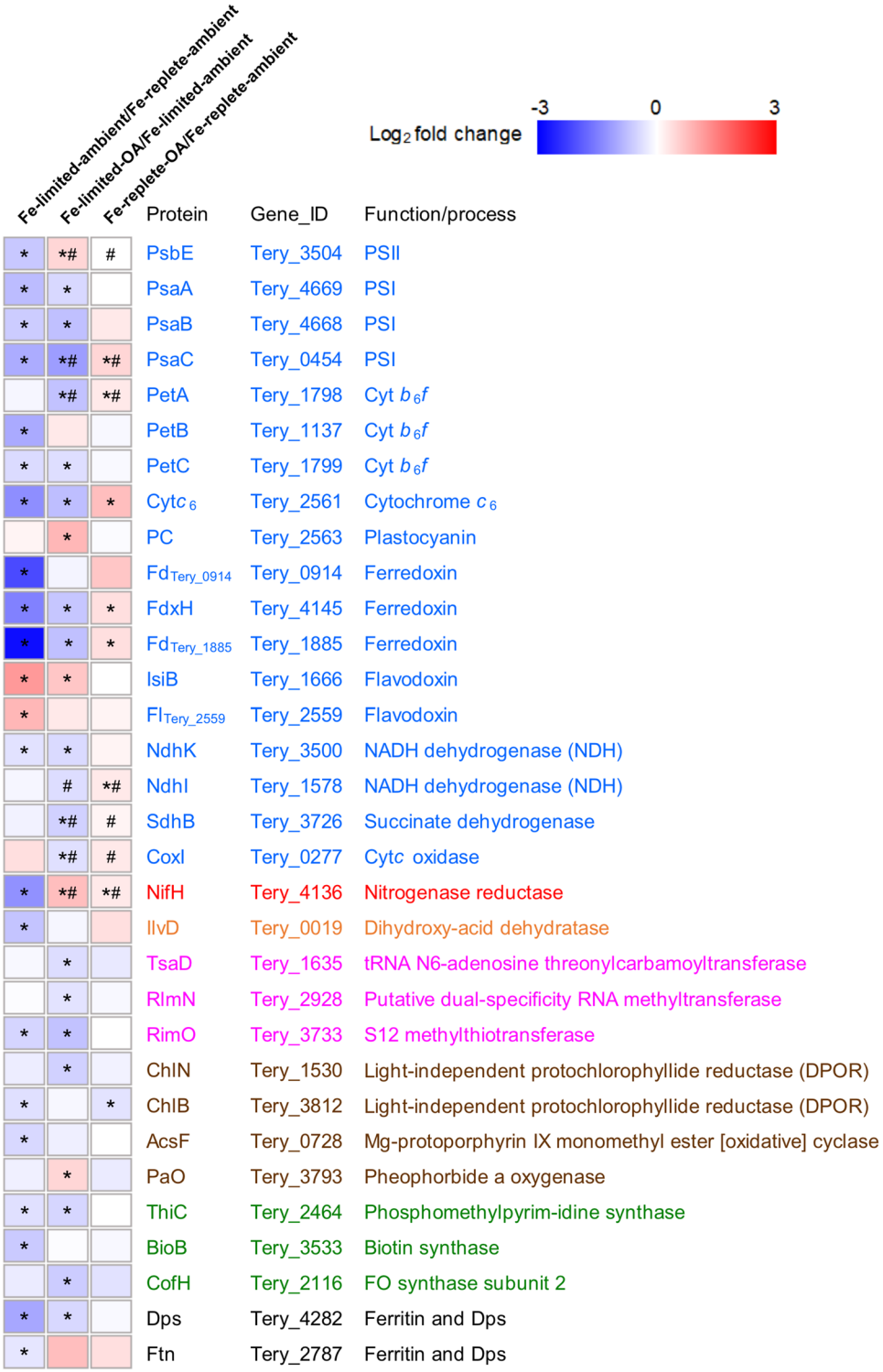

Fig. 3 Heatmap displaying the $\log_2$ fold change in protein expression between Fe (Fe-limited: 35 pM Fe'; Fe-replete: 925 pM Fe') and OA (ambient: 400 µatm CO_2, pH 8.02; acidified: 740 µatm CO_2, pH 7.81) treatments for Fe-containing and non-Fe substitution proteins that are involved in photosynthetic and respiratory electron transport (blue), N_2 fixation (red), amino acid biosynthesis (orange), RNA modification (purple), chlorophyll biosynthesis and degradation (brown), coenzyme synthesis (green), or Fe storage (black) in *T. erythraeum* strain IMS101. Asterisks (*) indicate significantly differentially expressed proteins (Student's *t*-test followed by Benjamini–Hochberg correction with 5% false discovery rate cutoff, fold changes of ≥ 1.2 or ≤ 0.83). Pound signs (#) denote data from Hong et al. (2017). Data of fold changes are presented in Table S2

respiration, and N_2 fixation, were significantly downregulated in Fe-limited *T. erythraeum* (Fig. 3, Fe-limited-ambient/Fe-replete-ambient). In addition, several Fe-containing proteins involved in chlorophyll biosynthesis and degradation, amino acid metabolism, RNA modification, coenzyme synthesis, and Fe storage were also significantly downregulated by Fe limitation (Fig. 3, Fe-limited-ambient/Fe-replete-ambient).

In response to OA, Fe-limited *T. erythraeum* significantly downregulated many Fe-containing proteins that are involved in photosynthetic and respiratory electron transport. These include PSI subunits (PsaA, PsaB, and PsaC), Cyt b_6f complexes (PetA and PetC), Cyt c_6, ferredoxin (FdxH and Fd_{Terry_1885}), NADH dehydrogenase complex (NdhK), succinate dehydrogenase (SdhB), and cytochrome *c* oxidase (CoxI) (Fig. 3, Fe-limited-OA/Fe-limited-ambient). Several non-Fe proteins in PSI (e.g., PsaJ), Cyt *c* oxidase II (e.g., CoxII), and NADH dehydrogenase complex (e.g., NdhA, NdhF, NdhB, NdhE, and NdhF4) were also significantly downregulated under acidified conditions (Table S3). In addition, Fe-containing proteins that are involved in chlorophyll synthesis (light-independent protochlorophyllide reductase subunit ChlN), RNA modification (tRNA N6-adenosine threonylcarbamoyltransferase TsaD, dual-specificity RNA methyltransferase RlmN, and S12 methylthiotransferase RimO), coenzyme synthesis (phosphomethylpyrim-idine synthase ThiC and FO synthase subunit 2 CofH), and Fe storage (ferritin and DPs Ftn) were significantly downregulated by OA (Fig. 3, Fe-limited-OA/Fe-limited-ambient).

In contrast, the Fe-containing PSII protein (PsbE), nitrogenase reductase (NifH), and pheophorbide a oxygenase (PaO, which is likely involved in chlorophyll degradation) were significantly upregulated by OA under Fe-limited condition (Fig. 3, Fe-limited-OA/Fe-limited-ambient). In addition, further PSII proteins, i.e., PsbP, PsbO, and Psb27 (Thornton et al. 2004; Mabbitt et al. 2009), were also markedly upregulated by 30, 60, and 20%, respectively (Table S3, Fe-limited-OA/Fe-limited-ambient), which was consistent with the upregulation of PsbE. The two nitrogenase protection proteins NifX and NifW (Kim and Burgess 1996; Hernandez et al. 2007) were upregulated by 30 and 40%, respectively (Table S3, Fe-limited-OA/Fe-limited-ambient), which is similar to the change of NifH under acidified conditions.

The increased PSII and decreased PSI together resulted in an increase in PSII:PSI ratio in Fe-limited *T. erythraeum* under acidified conditions. This proteomic result was confirmed by Western blotting of PsbA (the D1 protein of PSII) and PsaC (the core subunit of PSI). The analysis showed that the PSII:PSI ratio of Fe-limited *T. erythraeum*, as indicated by the PsbA:PsaC ratio, increased considerably from 1.53 ± 0.01 to 3.65 ± 0.06 as a result of acidification

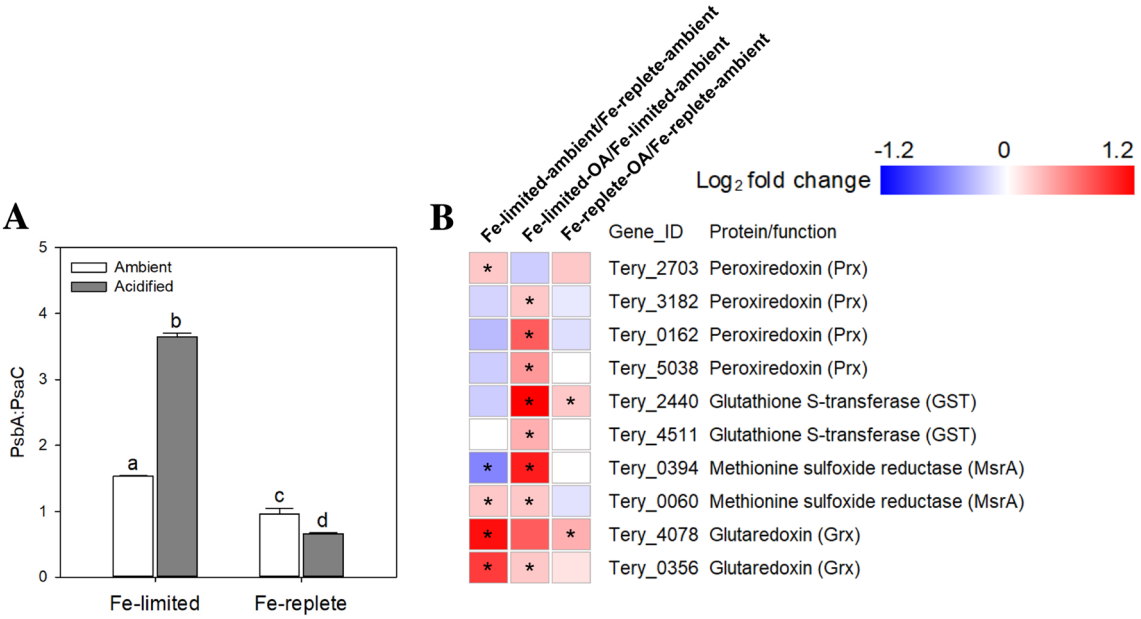

Fig. 4 **a** The PsbA:PsaC ratios in *T. erythraeum* strain IMS101 cultured under limiting (35 pM Fe') and replete (925 pM Fe') Fe concentrations under both ambient (400 µatm CO_2, pH 8.02) and acidified (740 µatm CO_2, pH 7.81) conditions. **b** The heatmap displays the $\log_2$ fold change in protein expression between Fe and OA treatments for proteins involved in the antioxidative defense of *T. erythraeum* strain IMS101. Error bars in **a** represent the SD of biological replicates ($n = 3$), and different superscript letters indicate significant differences ($p < 0.05$) among treatments (one-way ANOVA followed by Fisher LSD test). Asterisks (*) in **b** indicate significantly differentially expressed proteins (according to Student's *t*-test followed by Benjamini–Hochberg correction with 5% false discovery rate cutoff, fold changes of ≥ 1.2 or ≤ 0.83). Data of fold changes are presented in Table S4

(Fig. 4a). Increasing the PSII:PSI ratios under Fe-limited condition may increase the oxidative stress in *T. erythraeum* (Snow et al. 2015b). In agreement, several antioxidative proteins such as peroxiredoxin (Prx) family, glutathione S-transferase (GST), methionine sulfoxide reductase (MsrA), and glutaredoxin (Grx) were significantly upregulated by acidification under Fe-limited conditions (Fig. 4b, Fe-limited-OA/Fe-limited ambient).

Under Fe-replete conditions, acidification, however, did not downregulate Fe-containing proteins that were in lower abundance under Fe limitation. Instead, PsaC, PetA, Cytc_6, ferrodoxin (FdxH and Fd_{Terry_1885}), NdhI, and NifH were significantly upregulated by acidification, and SdhB and CoxI were slightly upregulated (Fig. 3, Fe-replete-OA/Fe-replete-ambient). In addition, the PSII:PSI ratios under both ambient and acidified conditions were < 1, and significantly decreased from 0.96 ± 0.08 to 0.66 ± 0.01 in response to OA (Fig. 4a). The number of antioxidative proteins (Prx-family, GST, MsrA, and Grx) induced by OA was much lower under Fe-replete conditions than under Fe-limited conditions (Fig. 4b).

Substitution by non-Fe-containing proteins under Fe stress

In marine phytoplankton, several Fe-containing proteins can be substituted by Fe-free equivalents under Fe stress, e.g., Cyt c_6 can be replaced by Cu-containing plastocyanin (PC) and ferredoxin can be replaced by flavodoxin (IsiB) (Leonhardt and Straus 1992; LaRoche et al. 1996; Behrenfeld and Milligan 2013). Indeed, Fe-limited *T. erythraeum* expressed much less ferredoxins compared to Fe-replete cells, and considerable upregulations of 130% and 80% were found in the substitution proteins IsiB and Tery_2559 (another flavodoxin), respectively (Fig. 3, Fe-limited-ambient/Fe-replete-ambient). Similarly, Cyt c_6 was significantly downregulated and PC was slightly but not significantly more abundant under Fe limitation (Fig. 3, Fe-limited-ambient/Fe-replete-ambient). With regard to the effects of OA in Fe-limited *T. erythraeum*, the Fe-containing Cyt c_6 and ferredoxin were both downregulated, whereas their corresponding substitution proteins PC and IsiB were significantly upregulated by 80% and 60%, respectively (Fig. 3, Fe-limited-OA/Fe-limited-ambient). The expressions of these substitution proteins, however, were not affected by OA in Fe-replete cells (Fig. 3, Fe-replete-acidified/Fe-replete-ambient).

Proteins involved in facilitating Fe acquisition

The Fe species that can be utilized by *Trichodesmium* include free dissolved inorganic Fe (ferrous, Fe^{2+} and ferric, Fe^{3+}), organically complexed Fe (e.g., siderophore-bound Fe), and particulate Fe (Chappell and Webb 2010; Kammler et al. 1993; Polyviou et al. 2018a; Rubin et al. 2011). Comparison of Fe-limited *T. erythraeum* with Fe-replete *T. erythraeum* under ambient conditions showed that FutA/IdiA (ferric uptake transporter A/iron deficiency-induced A, Tery_3377, Polyviou et al. 2018b) ratios and FutC (Tery_3222, an ATPase subunit, Polyviou et al. 2018b), which are involved in the transport of dissolved inorganic Fe^{2+} and Fe^{3+}, were upregulated by 190% and 80%, respectively (Fig. 5, Fe-limited-ambient/Fe-replete-ambient). In addition, proteins that may potentially be involved in Fe-siderophore uptake (e.g., Tery_3823, Tery_3825, and Tery_3826) as well as proteins with hemolysin-type calcium-binding domains (HTCaB) that may facilitate the absorption of dust Fe (Tery_1450, Tery_2055, Tery_0405, and Tery_0419) (Snow et al. 2015b; Polyviou et al. 2018a) were also significantly upregulated by 20–100% (Fig. 5, Fe-limited-ambient/Fe-replete-ambient).

Under Fe-limited conditions, OA significantly upregulated proteins involved in the acquisition of Fe-siderophore including TonB, ExbB, FhuD, Tery_3823, Tery_3825, and Tery_3826 (Fig. 5, Fe-limited-OA/Fe-limited-ambient). In addition, six of the 10 proteins with HTCaB-like domains (i.e., Tery_1450, Tery_2055, Tery_3467, Tery_3470, Tery_0424, and Tery_1355) were significantly upregulated, including alkaline phosphatase (Tery_3467) and proteins involved in the absorption of dust Fe (Tery_1450 and Tery_2055) (Snow et al. 2015b; Polyviou et al. 2018a) (Fig. 5, Fe-limited-OA/Fe-limited-ambient). In contrast, OA did not markedly affect the expression of Fe-uptake proteins in Fe-replete *T. erythraeum* (Fig. 5, Fe-replete-OA/Fe-replete-ambient).

Regulation of pigment synthesis

In cyanobacteria, the primary photosynthetic pigment Chl *a* and the accessory photosynthetic phycobilins (mainly phycocyanin and phycoerythrin) share a common tetrapyrrole biosynthetic pathway from 5-aminolevulinic acid (ALA) that involves approximately 20 enzymes (Fig. 6a) (Fenchel et al. 2012). Under Fe-limited conditions, OA significantly downregulated most of the enzymes involved in Chl *a* and phycobilin synthesis. These include HemC (hydroxymethylbilane synthase), HemE (uroporphyrinogen III decarboxylase), HemF (oxygen-dependent coproporphyrinogen III oxidase), $ChlH_{Tery\_0866}$ (Mg-chelatase subunit), ChlI (Mg-chelatase subunit), ChlN (light-independent protochlorophyllide reductase subunit), ChlP (geranylgeranyl diphosphate reductase), HemH (Fe-chelatase), PcyA (phycocyanobilin:ferredoxin oxidoreductase), and PebB (phycoerythrobilin:ferredoxin oxidoreductase). The following enzymes were slightly but not significantly downregulated: HemB (porphobilinogen synthase), $ChlH_{Tery\_3224}$ (Mg-chelatase), ChlD (Mg-chelatase), and

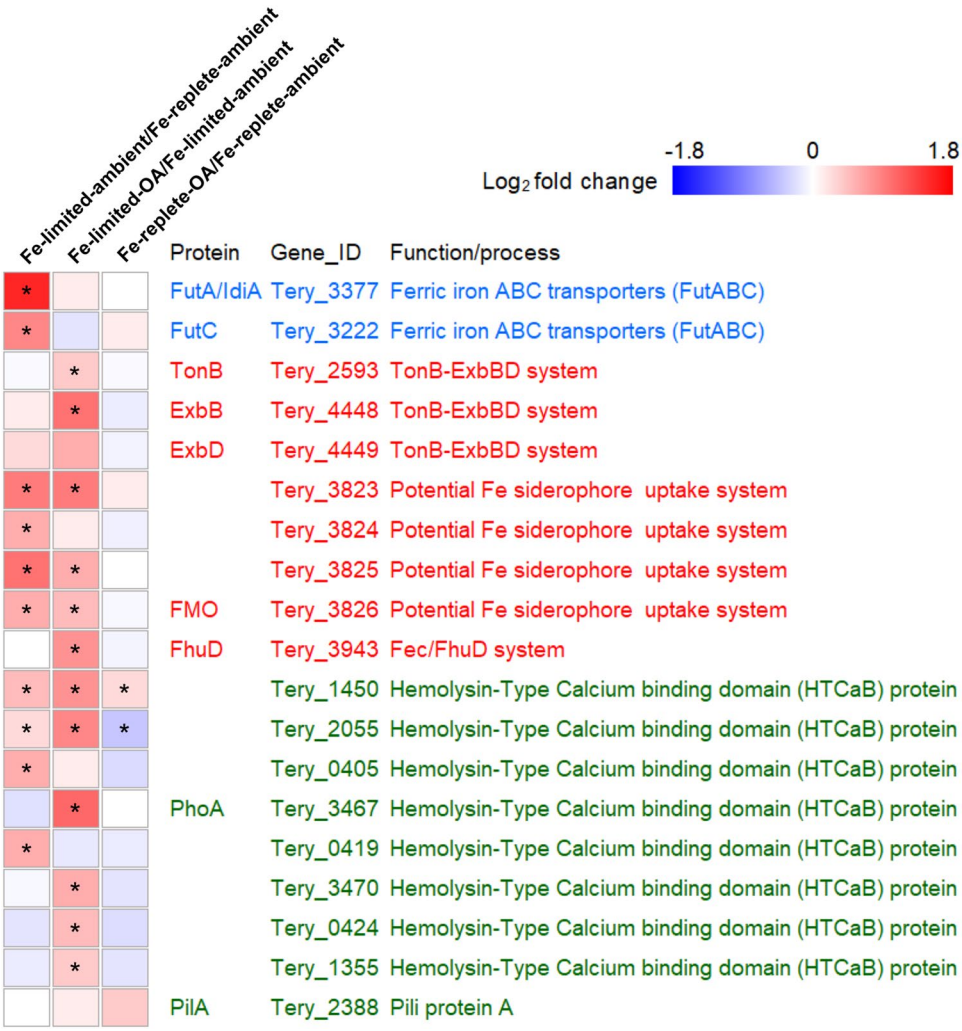

Fig. 5 The heatmap displaying the $\log_2$ fold change in protein expressions between Fe (Fe-limited: 35 pM Fe'; Fe-replete: 925 pM Fe') and OA (ambient: 400 µatm CO_2, pH 8.02; acidified: 740 µatm CO_2, pH 7.81) treatments for proteins that are involved in the acquisition of free dissolved inorganic Fe (blue), siderophore-bound Fe (red), or particulate Fe (green) in *T. erythraeum* strain IMS101. Asterisks (*) indicate significantly differentially expressed proteins (Student's *t*-test followed by Benjamini–Hochberg correction with 5% false discovery rate cutoff, fold changes of ≥ 1.2 or ≤ 0.83). Data of fold changes are presented in Table S5

AcsF (Mg-protoporphyrin IX monomethyl ester [oxidative] cyclase) (Fig. 6b, Fe-limited-OA/Fe-limited-ambient). Among these, both ChlN and AscF are Fe-containing proteins. The downregulation of these proteins involved in pigment synthesis was consistent with the reduced cellular Chl *a* content in acidified *T. erythraeum* under Fe-limited conditions (Fig. 1d).

Under Fe-replete conditions, acidification did not exert any noticeable effect on the expressions of most of the proteins involved in Chl *a* and phycobilin synthesis. The exception was that ChlI and ChlB were downregulated and ChlM (Mg-protoporphyrin IX methyl transferase) and PcyA were upregulated (Fig. 6b, Fe-replete-OA/Fe-replete-ambient). Consistently, the cellular Chl *a* content was not affected by OA in Fe-replete *T. erythraeum* (Fig. 1d).

Discussion

It is widely expected that OA will stimulate both growth and N_2 fixation of *Trichodesmium* since the downregulation of CCMs by high CO_2 can potentially save cellular energy and resources for other processes (Kranz et al. 2011; Luo et al. 2019). However, several recent field experiments have shown that acidification exerts either no obvious or even negative effects on N_2 fixation in *Trichodesmium* (Böttjer et al. 2014; Gradoville et al. 2014; Hong et al. 2017). In laboratory studies, Hong et al. (2017) reported that the negative effect of low pH offset the positive effect of high CO_2 and overall, OA had either no or a negative effect on growth and N_2 fixation of *T. erythraeum*. Similarly, Boatman et al. (2018), Eichner et al. (2014), and Kranz et al. (2009) also reported no significant effect of OA (720–1000 µatm CO_2 vs. 370–380 µatm CO_2) on the growth of *T. erythraeum* under nutrient-replete conditions. Moreover, Fe scarcity can amplify the negative effects of acidification (Shi et al. 2012; Hong et al. 2017).

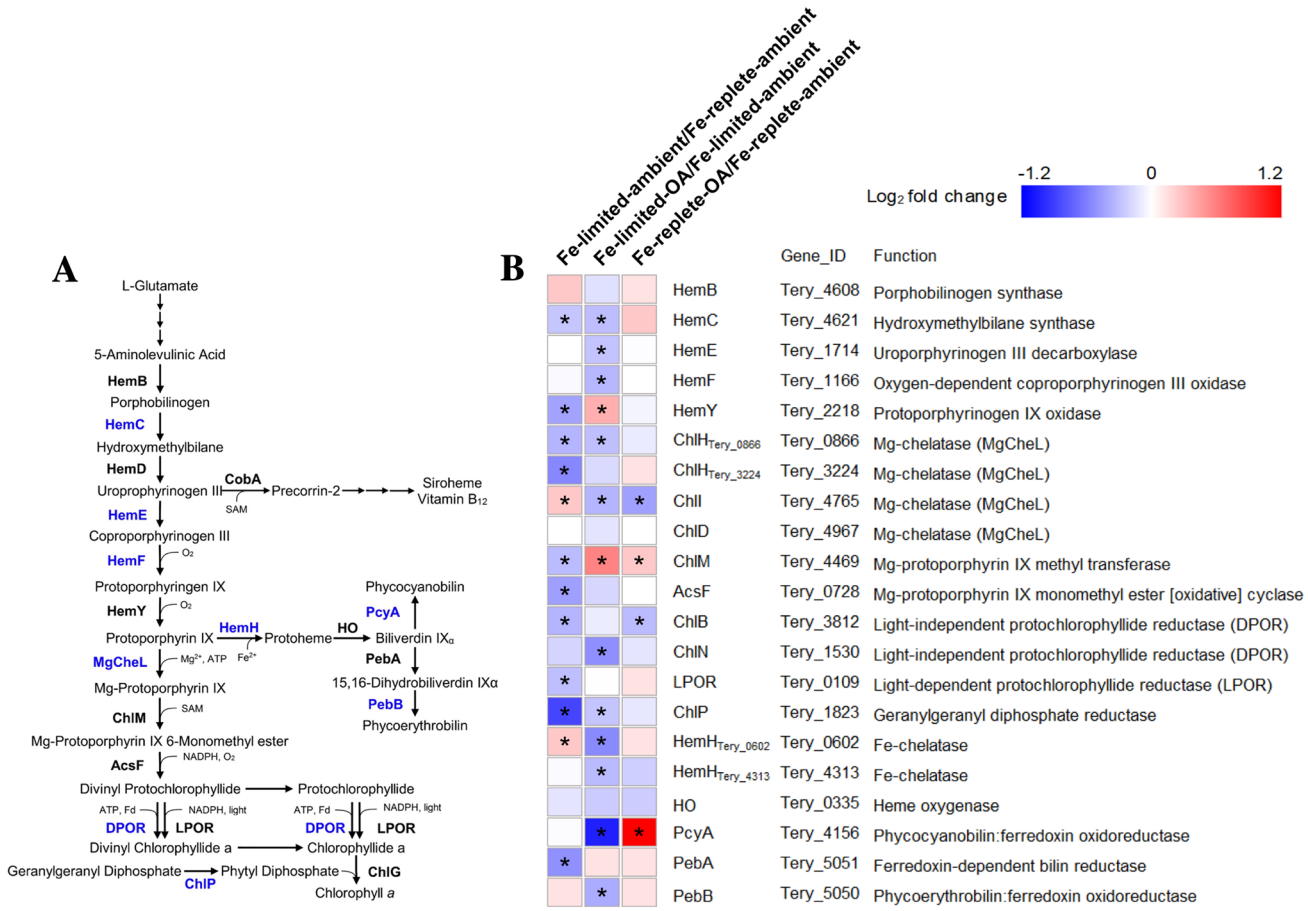

Fig. 6 **a** The de novo Chl *a* and phycobilin biosynthetic pathway. **b** The heatmap displays the $\log_2$ fold change in protein expression between Fe (Fe-limited: 35 pM Fe'; Fe-replete: 925 pM Fe') and OA (ambient: 400 µatm CO_2, pH 8.02; acidified: 740 µatm CO_2, pH 7.81) treatments for proteins that are involved in the Chl *a* and phycobilin biosynthesis in *T. erythraeum* strain IMS101. Asterisks (*) indicate significantly differentially expressed proteins (Student's *t*-test followed by Benjamini–Hochberg correction with 5% false discovery rate cutoff, fold changes of ≥ 1.2 or ≤ 0.83). Data of fold changes are presented in Table S6. Proteins in **a** that were significantly downregulated under acidified conditions in Fe-limited *T. erythraeum* strain IMS101 are indicated by names in blue, and proteins that were not significantly affected are indicated by names in black. Abbreviations: HemB, porphobilinogen synthase; HemC, hydroxymethylbilane synthase; HemE, uroporphyrinogen III decarboxylase; HemF, oxygen-dependent coproporphyrinogen III oxidase; HemY, protoporphyrinogen IX oxidase; $ChlH_{Tery\_0866}$, $ChlH_{Tery\_3224}$, ChlI, and ChlD, Mg-chelatase (MgCheL); ChlM, Mg-protoporphyrin IX methyl transferase; AcsF, Mg-protoporphyrin IX monomethyl ester [oxidative] cyclase; ChlB and ChlN, light-independent protochlorophyllide reductase (DPOR); LPOR, light-dependent protochlorophyllide reductase (LPOR); ChlP, geranylgeranyl diphosphate reductase; $HemH_{Tery\_0602}$ and $HemH_{Tery\_4313}$, Fe-chelatase; HO, Heme oxygenase; PcyA, phycocyanobilin:ferredoxin oxidoreductase; PebA, ferredoxin-dependent bilin reductase; PebB, phycoerythrobilin:ferredoxin oxidoreductase

The present study showed that for a given Fe' (i.e., constant Fe bioavailability), OA led to a significant decrease in growth and N_2 fixation rates of *T. erythraeum* under both Fe-replete and Fe-limited conditions, and the negative effects were far more obvious in Fe-limited *T. erythraeum* (Fig. 1a, b). This matches previous observations (Shi et al. 2012; Hong et al. 2017). In addition, the C-fixation rates decreased in response to OA, which was statistically significant in Fe-limited *T. erythraeum* (Fig. 1c). Since low pH reduced the N_2-fixation efficiency of nitrogenase, the N_2-fixation rate of *T. erythraeum* significantly decreased despite enhanced nitrogenase expression (Shi et al. 2012). This increase in the Fe-rich nitrogenase came at the expense of a downregulation of photosynthetic and respiratory electron transport proteins as well as other intracellular sources in Fe-limited *T. erythraeum* (Fig. 3, Fe-limited-OA/Fe-limited-ambient), as previously reported (Hong et al. 2017). This Fe reallocation, however, was not pronounced in Fe-replete *T. erythraeum* (Fig. 3, Fe-replete-OA/Fe-replete-ambient). The negative effects of OA were thus more substantial under Fe-limited conditions.

In marine phytoplankton, it has been found that under Fe stress, Cyt c_6 (containing 1 heme center) can be

replaced by Cu-dependent plastocyanin, and ferredoxin (containing a 2Fe-2S center) can be replaced by the non-metalloprotein flavodoxin (IsiB) (Behrenfeld and Milligan 2013). In particular, the expression of IsiB has been frequently used as Fe-stress biomarker in field studies (Chappell and Webb 2010; Chappell et al. 2012). Compared to Fe-replete-ambient cells, the expression of Cyt c_6 and ferredoxin decreased more dramatically in Fe-limited-OA cells than in the Fe-limited-ambient cells (see Table S7). The same pattern was observed for other photosynthetic and electron transport proteins, e.g., PSI and Cyt b_6f (Table S7). These results indicate that in the already Fe-limited *T. erythraeum*, the reallocation of Fe to nitrogenase, which was significantly upregulated in response to OA, further impaired the Fe requirement of other key cellular processes. In addition, the substitution proteins PC and IsiB were induced more markedly in Fe-limited-OA cells compared to Fe-limited-ambient cells (Table S7). In summary, changes in the expression of these proteins suggest that under Fe-limited conditions, OA caused an increasing shortage of Fe in pathways (e.g., photosynthesis and respiration) that yielded Fe to nitrogenase in *T. erythraeum*, thus inducing Fe-economic strategies (e.g., increased expression of PC and IsiB).

It has been reported that the Fe-stress protein IsiA/B can be induced under oxidative stress and as a result of Fe limitation (Yousef et al. 2003; Havaux et al. 2005; Kojima et al. 2006), and Fe deficiency can cause oxidative stress in oxygenic photosynthetic cyanobacteria (Latifi et al. 2005). Due to the strong interrelationship between Fe deficiency and oxidative stress in oxygenic photosynthetic organisms, ROS might be the superior trigger for the expression of IsiA/B under Fe-limited conditions (Michel and Pistorius 2004). In the current study, an increase in several antioxidative proteins was observed under OA in Fe-limited *T. erythraeum*, including Prxs, GSTs, MsrAs, and Grxs (Fig. 4b). Prxs (alkylhydroperoxidases) represent a group of ubiquitous antioxidative proteins that catalyze the reduction of H_2O_2, alkyl hydroperoxides, and peroxynitrite (Cui et al. 2012; Latifi et al. 2009). GSTs are involved in the antioxidative response and in restoring the activity of oxidized Prxs (Hayes et al. 2005). MsrA proteins are prominent antioxidative enzymes that indirectly combat oxidative stress by repairing oxidized proteins (Sreekumar et al. 2011). Increased expression of these antioxidative proteins in response to OA together with the induction of IsiB protein in Fe-limited *T. erythraeum,* but not in Fe-replete cells, suggest that OA may enhance the already detrimental effects of Fe limitation, e.g., by increasing oxidative stress, in Fe-limited *T. erythraeum*.

It has been shown that Fe deficiency often induces chlorosis, which is attributed to the decrease in photosynthetic pigments (e.g., chlorophyll and phycobilins) (Davey and Geider 2001; Guikema and Sherman 1983; Moseley et al. 2002). Chl *a* is the only known chlorophyll in *Trichodesmium* (Li and Chen 2015). The current study demonstrated that Chl *a* content and pigment synthesis were almost not affected by OA in Fe-replete *T. erythraeum* (Figs. 1d and 6, Fe-replete-OA/Fe-replete-ambient). In contrast, acidification significantly lowered the content of Chl *a* along with many enzymes involved in pigment synthesis in Fe-limited *T. erythraeum* (Figs. 1d and 6, Fe-limited-OA/Fe-limited-ambient). This may result in a lower capability to absorb light and conduct photosynthesis and N_2 fixation.

PSI and PSII are the main chlorophyll-binding units, and it has been reported that PSI binds more chlorophyll molecules than PSII (96 vs. 26) in cyanobacteria (Jordan et al. 2001; Zouni et al. 2001). In addition, the synthesis of both PSI and PSII mainly uses newly made and recycled chlorophyll, respectively, which suggests that the de novo chlorophyll synthesis reflects the cellular demand of PSI (Kopečná et al. 2012; Sobotka 2014). The present study found a considerable decline in PSI proteins (PsaA, PsaB, and PsaC) under OA in Fe-limited *T. erythraeum* (Figs. 3 and 4a, Fe-limited-OA/Fe-limited-ambient), which is consistent with the downregulation of pigment biosynthesis (Fig. 6, Fe-limited-OA/Fe-limited-ambient). As a result, or due to a reduction in light capture and electron transport capability, Fe-limited cells significantly decreased photosynthetic C fixation, growth, and N_2 fixation in response to OA (Fig. 1).

When Fe was sufficient, the upregulation of Fe-rich nitrogenase, as a compensation for the reduced efficiency of nitrogenase, did not impair the expression of PSI proteins or enzymes involved in pigment synthesis (Figs. 3 and 6, Fe-replete-OA/Fe-replete-ambient). This indicates a lack of Fe reallocation from other biological pathways to nitrogenase. Therefore, photosynthetic C fixation was not affected even though both growth and N_2-fixation rates were slightly decreased (Fig. 1). The results further supported that Fe limitation amplified the negative effects of OA on *T. erythraeum*.

It has been estimated that C and N_2 fixations of *Trichodesmium* require ATP:NADPH + H^+ ratios of 3:2 and 2:1, respectively, which indicates a higher requirement for ATP than for NADPH (Kranz et al. 2011). In general, linear photosynthetic electron transport (LET, electron transfer from PSII to PSI) yields an ATP:NADPH + H^+ ratio of approximately 1 (Kranz et al. 2011). An additional source of ATP is thus required to satisfy the energy demand during C and N_2 fixation. In cyanobacteria, this additional ATP can be derived from a number of alternative electron transfer pathways, including cyclic photosynthetic electron transport around PSI, a water–water electron cycle from PSII to water via midstream oxidase (PSII-MOX), and electron transport from PSII to respiratory terminal oxidases (PSII-RTO) (Bailey et al. 2008; Behrenfeld et al. 2008; Behrenfeld

and Milligan 2013). The PSI cyclic pathway (57-63 Fe) requires significantly more Fe than both PSII-MOX (36 Fe) and PSII-RTO (18 Fe) pathways (Behrenfeld and Milligan 2013). Consequently, under Fe-sufficient conditions, when the PSII:PSI ratio is < 1, the additional ATP required is mainly supplied by the cyclic PSI pathway; however, under low-Fe conditions, when the ratio is > 1, the role of alternative electron flows (e.g., PSII-MOX and/or PSII-RTO) in supplying ATP may increase (Behrenfeld and Milligan 2013; Snow et al. 2015b). In the present study, *T. erythraeum* had PSII:PSI ratios of < 1 and > 1 under Fe-replete and Fe-limited conditions, respectively (Fig. 4a), which was consistent with the observation reported in Snow et al. (2015b). Thus, although this study provided no direct measurements, the observed PSII:PSI ratios indicate that under Fe-replete conditions, the additional ATP in *T. erythraeum* was likely supplied by the highly Fe-demanding cyclic PSI pathway. In contrast, under Fe limitation, while cyclic PSI likely still remains important, there is an increased reliance on the more Fe-economic alternative electron flow to supply additional ATP, e.g., PSII-MOX and/or PSII-RTO pathways (Snow et al. 2015b). It should be noted that MOX genes have not been identified in the genome of *T. erythraeum* strain IMS101, which does not support the existence of PSII-MOX electron flow. However, in the current study, two RTO enzymes (i.e., COX1 and COX2, Snow et al. 2015b) were slightly upregulated under Fe-limited conditions (Tables S2 and S3, Fe-limited-ambient/Fe-replete-ambient), thus suggesting the possibly increased reliance on the PSII-RTO pathway under Fe limitation.

The PSII:PSI ratio of *T. erythraeum* was also found to be affected by OA in the current study, and these effects differed under Fe-replete and Fe-limited conditions. As previously reported (Shi et al. 2012), the ratio decreased significantly in Fe-replete *T. erythraeum* but increased significantly in Fe-limited cells under acidified conditions (Fig. 4A). When Fe is sufficient, *T. erythraeum* may increase the cyclic electron transport around PSI (low PSII:PSI ratio) to enhance ATP production in an effort to cope with the OA imposed stress (Hong et al. 2017). However, under Fe-limited conditions, although the induction of IsiB by OA might help increase cyclic electron transport (Hagemann et al. 2002), it is unlikely that the Fe-demanding PSI cyclic pathway would increase for the additional ATP supply in response to OA. In addition, acidification also significantly downregulated several RTO related enzymes (e.g., Fe-containing CoxI, CoxII, and Cyt b_6f) (Fig. 3 and Tables S2 and S3, Fe-limited-OA/Fe-limited-ambient) in Fe-limited *T. erythraeum*. This suggests that the capability of the PSII-RTO pathway to supply additional ATP also decreased. Therefore, the additional ATP supply in Fe-limited *T. erythraeum* could be hampered by OA, which consequently resulted in lower growth and N_2-fixation rates.

Under Fe-limited conditions, marine phytoplankton are known to induce the expression of a series of proteins involved in the acquisition of various Fe species, including dissolved inorganic Fe, organically complexed Fe, and particulate Fe (Hernández-Prieto et al. 2012; Peuser et al. 2011; Snow et al. 2015b; Zappa and Bauer 2017). In the present study, although OA intensified the already adverse effects of Fe shortage in *T. erythraeum*, no changes were observed in the expression of dissolved free Fe^{3+} (FutABC) acquisition systems (Fig. 5). However, it should be noted that in the current study, a constant Fe' (bioavailable inorganic Fe concentration) was maintained under both ambient and acidified conditions through the control of the total dissolved Fe concentration in the EDTA-buffered growth medium. It is possible that the expression of these transporters was regulated by Fe' concentrations, and hence, their expression in *T. erythraeum* remained unaffected by OA in this study. In the future ocean, on the one hand, the bioavailability of dissolved Fe may decline in response to OA (Shi et al. 2010); on the other hand, acidification will likely increase the dissolution of particulate Fe (Millero et al. 2009). The expression of the transporters of dissolved Fe in *T. erythraeum* under OA may therefore largely depend on the bioavailability of dissolved Fe concentrations in seawater as a net result of the influence of OA on the different chemical forms of Fe.

In addition to dissolved inorganic Fe, it has been shown that *Trichodesmium* colonies are able to utilize dust particles as Fe source (Rubin et al. 2011; Basu and Shaked 2018). The cell-surface processes for Fe-siderophore uptake may accelerate this dissolution of Fe from dust (Basu and Shaked 2018; Polyviou et al. 2018a). Proteins with a HTCaBs domain, which occur in tandem repeats to form a parallel β-roll structure, have been reported to aid the mobilization of Fe from dust (Brahamsha 1996; Hoiczyk and Baumeister 1997; Polyviou et al. 2018a). In the present study, the acquisition systems of both organically complexed Fe and particulate Fe (e.g., TonB-ExbBD, Fec/FhuD, Tery_3823-3826, and HTCaBs proteins) were significantly upregulated in response to OA in Fe-limited *T. erythraeum* (Fig. 5). These results suggest that Fe limitation enhanced the acquisition mechanisms for all possible Fe species, including both Fe-siderophore and particulate Fe, to alleviate Fe scarcity in response to OA. In the future ocean, dust depositions may increase and hence become an increasingly important source of Fe for *Trichodemium* (Mahowald et al. 2009). Further studies are required to elucidate how OA may affect the utilization of this Fe source by *Trichodesmium* through abiotic and/or biotic dust dissolution (Basu and Shaked 2018).

In summary, our study demonstrates that the major metabolic processes responded differently to OA in Fe-replete and Fe-limited *T. erythraeum* (Fig. 7). Under Fe-replete conditions, *T. erythraeum* demonstrated an upregulation of PSI and several electron transport proteins in response

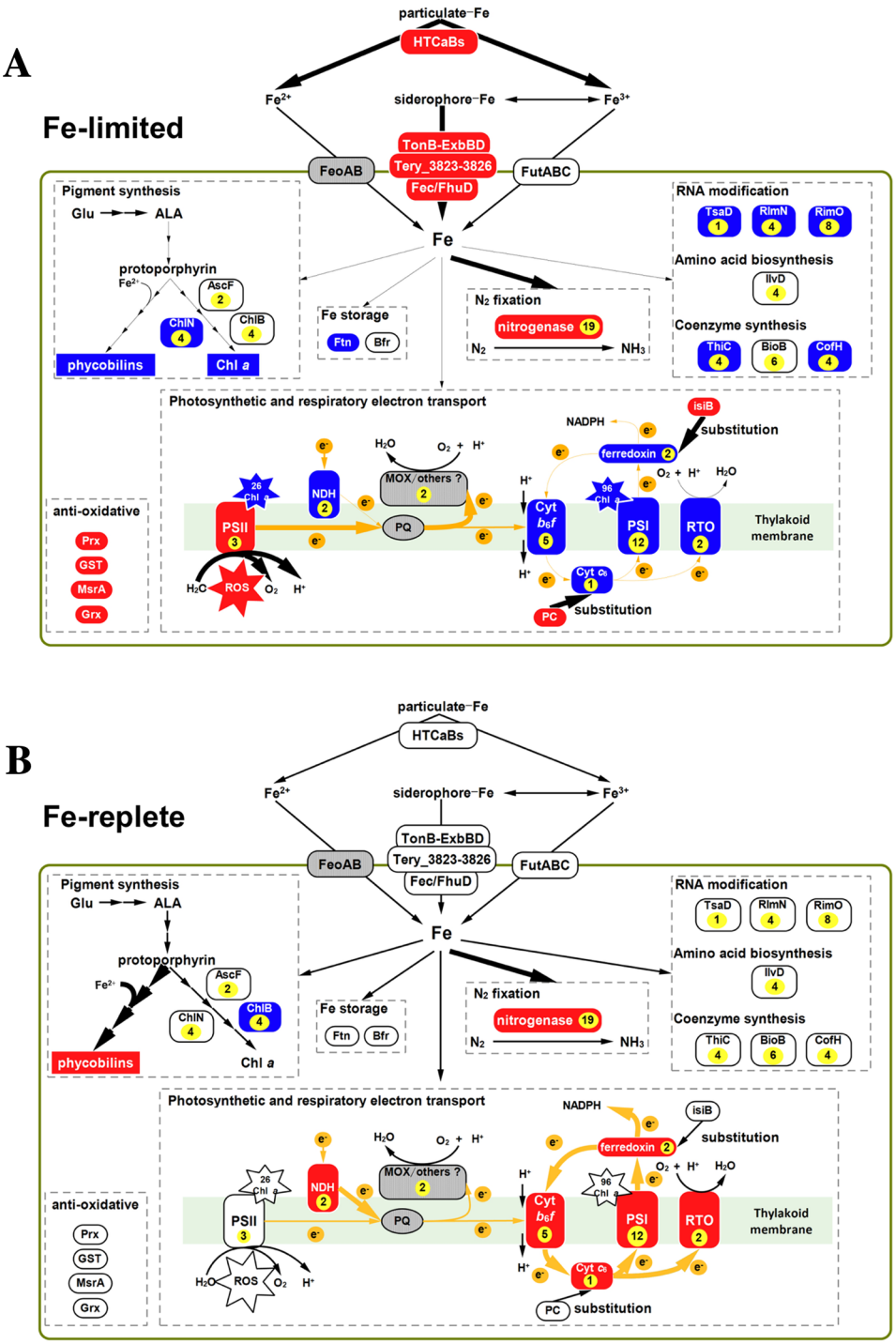

Fig. 7 Schematic representation of changes in the abundance of key proteins involved in Fe acquisition, pigment synthesis, Fe storage, N_2 fixation, RNA modification, amino acid biosynthesis, coenzyme synthesis, photosynthetic and respiratory electron transport, and antioxidative defense in **a** Fe-limited and **b** Fe-replete *T. erythraeum* strain IMS101 in response to OA. Yellow circles with numbers denote Fe-containing proteins and Fe atoms per monomer of the proteins. Red: upregulated; blue: downregulated; white: unchanged; gray: undetected or unidentified. Increased/decreased thickness and size of orange and black arrows indicate increased/decreased electron flow and pathways, respectively

to OA. This enhanced the electron transport around the PSI cyclic pathway for additional ATP production to fulfill the increasing demand for energy to cope with the stress imposed by low pH. In contrast, under Fe-limited conditions, the enhanced expression of Fe-rich nitrogenase, as a compensation for the suppressed N_2-fixation efficiency under OA, caused the reallocation of Fe from PSI, electron transport proteins, and pigment synthetic enzymes to nitrogenase. This significantly obstructed the energy production and thus considerably reduced both N_2- and C-fixation rates. To still fulfill the increased Fe requirement of nitrogenase under OA, *T. erythraeum* adopted Fe-economic strategies, which include the increase in non-Fe substitution proteins (e.g., flavodoxin and PC). Furthermore, Fe-limited *T. erythraeum* upregulated its acquisition mechanisms for various Fe species (e.g., Fe-siderophore

and particulate Fe) in response to OA. This study provides mechanistic insight into how the prominent marine diazotroph *Trichodesmium* may perform in a more acidic and Fe-limited future ocean.

Acknowledgements The authors thank Z. Wen for his help with seawater collection from the South China Sea. The authors also thank two anonymous reviewers for helpful and constructive comments on the manuscript. This work was funded by the National Key R&D Program of China (No. 2016YFA0601203), and the National Science Foundation of China (Nos. 31861143022, 41890802, and 41721005).

Compliance with ethical standards

Conflict of interest The authors declare that they have no conflicts of interest.

References

Bailey S et al (2008) Alternative photosynthetic electron flow to oxygen in marine *Synechococcus*. Biochim Biophys Acta 1777:269–276

Basu S, Shaked Y (2018) Mineral iron utilization by natural and cultured *Trichodesmium* and associated bacteria. Limnol Oceanogr 63:2307–2320

Behrenfeld MJ, Milligan AJ (2013) Photophysiological expressions of iron stress in phytoplankton. Annu Rev Mar Sci 5:217–246

Behrenfeld MJ, Halsey KH, Milligan AJ (2008) Evolved physiological responses of phytoplankton to their integrated growth environment. Philos Trans R Soc B 363:2687–2703

Berman-Frank I, Lundgren P, Chen YB, Küpper H, Kolber Z, Bergman B, Falkowski P (2001) Segregation of nitrogen fixation and oxygenic photosynthesis in the marine cyanobacterium *Trichodesmium*. Science 294:1534–1537

Berman-Frank I, Quigg A, Finkel ZV, Irwin AJ, Haramaty L (2007) Nitrogen-fixation strategies and Fe requirements in cyanobacteria. Limnol Oceanogr 52:2260–2269

Boatman TG, Oxborough K, Gledhill M, Lawson T, Geider RJ (2018) An integrated response of *Trichodesmium erythraeum* IMS101 growth and photo-physiology to iron, CO_2, and light intensity. Front Microbiol 9:624

Böttjer D, Karl DM, Letelier RM, Viviani DA, Church MJ (2014) Experimental assessment of diazotroph responses to elevated seawater pCO_2 in the North Pacific Subtropical Gyre. Glob Biogeochem Cycle 28:601–616

Brahamsha B (1996) An abundant cell-surface polypeptide is required for swimming by the nonflagellated marine cyanobacterium *Synechococcus*. Proc Natl Acad Sci USA 93:6504–6509

Brand LE (1991) Minimum iron requirements of marine phytoplankton and the implications for the biogeochemical control of new production. Limnol Oceanogr 36:1756–1771

Caldeira K, Wickett ME (2003) Oceanography: anthropogenic carbon and ocean pH. Nature 425:365

Capone DG (1993) Determination of nitrogenase activity in aquatic samples using the acetylene reduction procedure. In: Kemp PF, Sherr B, Sheer E, Cole J (eds) Handbook of methods in aquatic microbial ecology. Lewis Publisher, New York, pp 621–631

Chappell P, Webb E (2010) A molecular assessment of the iron stress response in the two phylogenetic clades of *Trichodesmium*. Environ Microbiol 12:13–27

Chappell PD, Moffett JW, Hynes AM, Webb E (2012) Molecular evidence of iron limitation and availability in the global diazotroph *Trichodesmium*. ISME J 6:1728–1739

Cui H, Wang Y, Wang Y, Song Q (2012) Genome-wide analysis of putative peroxiredoxin in unicellular and filamentous cyanobacteria. BMC Evol Biol 12:220

Davey M, Geider RJ (2001) Impact of iron limitation on the photosynthetic apparatus of the diatom *Chaetoceros Muelleri* (bacillariophyceae). J Phycol 37:987–1000

Dickson AG, Millero FH (1987) A comparison of the equilibrium constants for the dissociation of carbonic acid in seawater media. Deep Sea Res 34:1733–1743

Doney SC, Fabry VJ, Feely RA, Kleypas JA (2009) Ocean acidification: the other CO_2 problem. Annu Rev Mar Sci 1:161–192

Eichner M, Kranz SA, Rost B (2014) Combined effects of different CO_2 levels and N sources on the diazotrophic cyanobacterium *Trichodesmium*. Physiol Plant 152:316–330

Fenchel T, King GM, Blackburn TH (2012) Bacterial biogeochemistry, 3rd edn. Academic Press, Boston

Galloway JN, Schlesinger WH, Levy H, Michaels AF, Schnoor JL (1995) Nitrogen fixation: anthropogenic enhancement-environmental response. Glob Biogeochem Cycle 9:235–252

Gradoville MR, White AE, Böttjer D, Church MJ, Letelier RM (2014) Diversity trumps acidification: lack of evidence for carbon dioxide enhancement of *Trichodesmium* community nitrogen or carbon fixation at Station ALOHA. Limnol Oceanogr 59:645–659

Gruber N, Sarmiento JL (1997) Global patterns of marine nitrogen fixation and denitrification. Glob Biogeochem Cycle 11:235–266

Guikema JA, Sherman LA (1983) Organization and function of Chlorophyll in membranes of cyanobacteria during iron starvation. Plant Physiol 73:250–256

Hagemann M, Jeanjean R, Fulda S, Havaux M, Joset F, Erdmann N (2002) Flavodoxin accumulation contributes to enhanced cyclic electron flow around photosystem I in salt-sressed cells of *Synechocystis* sp. Strain PCC 6803. Physiol Plant 105:670–678

Havaux M, Guedeney G, Hagemann M, Yeremenko N, Matthijs HCP, Jeanjean R (2005) The chlorophyll-binding protein IsiA is inducible by high light and protects the cyanobacterium *Synechocystis* PCC6803 from photooxidative stress. FEBS Lett 579:2289–2293

Hayes JD, Flanagan JU, Jowsey IR (2005) Glutathione transferases. Annu Rev Pharmacol 45:51–88

Hernandez JA, Igarashi RY, Curatti L, Dean DR, Ludden PW, Rubio LM (2007) NifX and NIfEN exchange NifB cofactor and the VK-cluster, a newly isolated intermediate of the iron-molybdenum cofactor biosynthetic pathway. Mol Microbiol 63:177–192

Hernández-Prieto MA, Schön V, Georg J, Barreira L, Varela J, Hess WR, Futschik ME (2012) Iron deprivation in *Synechocystis*: inference of pathways, non-coding RNAs, and regulatory elements from comprehensive expression profiling. Genes Genomes Genet 2:1475–1495

Hochberg Y (1995) Controlling the false discovery rate: a practical and powerful approach to multiple testing. J R Stat Soc B 57:289–300

Hoiczyk E, Baumeister W (1997) Oscillin, an extracellular, Ca^{2+}-binding glycoprotein essential for the gliding motility of cyanobacteria. Mol Microbiol 26:699–708

Hong H et al (2017) The complex effects of ocean acidification on the prominent N_2-fixing cyanobacterium *Trichodesmium*. Science 356:527–531

Hutchins DA et al (2007) CO_2 control of *Trichodesmium* N_2 fixation, photosynthesis, growh rates, and elemental ratios: implications for past, present, and future ocean biogeochemistry. Limnol Oceanogr 52:1293–1304

Jiann K-T, Wen L-S (2012) Distribution and lability of dissolved iron in surface waters of marginal seas in southeastern Asia. Estuar Coast Shelf Sci 100:142–149

Jordan P, Fromme P, Witt HT, Klukas O, Saenger W, Krauss N (2001) Three-dimensional structure of cyanobacterial photosystem I at 2.5 A resolution. Nature 411:909–917

Kammler M, Schön C, Hantke K (1993) Characterization of the ferrous iron uptake system of *Escherichia coli*. J Bacteriol 175:6212–6219

Kim S, Burgess BK (1996) Evidence for the direct interaction of the nifH gene product with the MoFe protein. J Biol Chem 271:9764–9770

Kojima K, Suzuki-Maenaka T, Kikuchi T, Nakamoto H (2006) Roles of the cyanobacterial *isiABC* operon in protection from oxidative and heat stresses. Physiol Plantarum 128:507–519

Kopečná J, Komenda J, Bučinská L, Sobotka R (2012) Long-term acclimation of the cyanobacterium *Synechocystis* sp. PCC 6803 to high light is accompanied by an enhanced production of chlorophyll that is preferentially channeled to trimeric photosystem I. Plant Physiol 160:2239–2250

Kranz SA, Sueltemeyer D, Richter K-U, Rost B (2009) Carbon acquisition by *Trichodesmium*: the effect of pCO_2 and diurnal changes. Limnol Oceanogr 54:548–559

Kranz SA, Levitan O, Richter K, Prasil O (2010) Combined effects of CO_2 and light on the N_2-fixing cyanobacterium *Trichodesmium* IMS101: physiological Responses. Plant Physiol 154:334–345

Kranz SA, Eichner M, Rost B (2011) Interactions between CCM and N_2 fixation in *Trichodesmium*. Photosynth Res 109:73–84

Kustka AB, Sañudo-Wilhelmy SA, Carpenter EJ, Capone D, Burns J, Sunda WG (2003) Iron requirements for dinitrogen- and ammonium-supported growth in cultures of *Trichodesmium* (IMS 101): comparison with nitrogen fixation rates and iron: carbon ratios of field populations. Limnol Oceanogr 48:1869–1884

LaRoche J, Boyd PW, McKay RML, Geider RJ (1996) Flavodoxin as an in situ marker for iron stress in phytoplankton. Nature 382:802–804

Latifi A, Jeanjean R, Lemeille S, Havaux M, Zhang CC (2005) Iron stravation leads to oxidative stress in *Anabaena* sp. strain PCC 7120. J Bacteriol 187:6596–6598

Latifi A, Ruiz M, Zhang CC (2009) Oxidative stress in cyanobacteria. FEMS Microbiol Rev 33:258–278

Leonhardt K, Straus NA (1992) An iron stress operon involved in photosynthetic electron transport in the marine cyanobacterium *Synechococcus* sp. PCC 7002. J Gen Microbiol 138:1613–1621

Levitan O et al (2007) Elevated CO_2 enhances nitrogen fixation and growth in the marine cyanobacterium *Trichodesmium*. Glob Chang Biol 13:531–538

Li Y, Chen M (2015) Novel chlorophylls and new directions in photosynthesis research. Funct Plant Biol 42:493–501

Luo Y-W, Shi D, Kranz SA, Hopkinson BM, Hong H, Shen R, Zhang F (2019) Reduced nitrogenase efficiency domniates response of the globally important nitrogen fixer *Trichodesmium* to ocean acidification. Nat Commun. https://doi.org/10.1038/s41467-019-09554-7

Mabbitt PD, Rautureau GJ, Day CL, Wilbanks SM, Eaton-Rye JJ, Hinds MG (2009) Solution structure of Psb27 from cyanobacterial photosystem II. Biochem 248:8771–8773

Mahaffey C, Michaels AF, Capone DG (2005) The conundrum of marine N_2 fixation. Am J Sci 305:546–595

Mahowald NM et al (2009) Atmospheric iron deposition: global distribution, variability, and human perturbations. Ann Rev Mar Sci 1:245–278

Mehrbach C, Culberso CH, Hawley JE, Pytkowic RM (1973) Measurement of apparent dissociation constants of carbonic acid in seawater at atmospheric pressure. Limnol Oceanogr 18:897–907

Michel K-P, Pistorius EK (2004) Adaptation of the photosynthetic electron transport chain in cyanobacteria to iron deficiency: the function of IdiA and IsiA. Physiol Plant 120:36–50

Millero FJ, Woosley R, Ditrolio B, Waters J (2009) Effects of ocean acidification on the speciation of metals in seawater. Oceanography 22:72–85

Moseley JL, Allinger T, Herzog S, Hoerth P, Wehinger E, Merchant SS, Hippler M (2002) Adaptation to Fe-deficiency requires remodeling of the photosynthetic apparatus. EMBO J 21:6709–6720

Peuser V, Metz S, Klug G (2011) Response of the photosynthetic bacterium *Rhodobacter sphaeroides* to iron limitation and the role of a Fur orthologue in this response. Environ Microbiol Rep 3:397–404

Pierrot D, Lewis E, Wallace D (2006) MS Excel program developed for CO_2 system calculations. Carbon Dioxide Information Analysis Center, Oak Ridge National Laboratory, US Department of Energy, Oak Ridge

Polyviou D, Baylay AJ, Hitchcock A, Robidart J, Moore CM, Bibby TS (2018a) Desert dust as a source of iron to the globally important diazotroph *Trichodesmium*. Front Microbiol 8:2683

Polyviou D et al (2018b) Structural and functional characterization of IdiA/FutA (Tery_3377), an iron binding protein from the ocean diazotroph *Trichodesmium erythraeum*. J Biol Chem 293:18099–18109

Richier S, Macey AI, Pratt NJ, Honey DJ, Moore CM, Bibby TS (2012) Abundances of iron-binding photosynthetic and nitrogen-fixing proteins of *Trichodesmium* both in culture and in situ from the North Atlantic. PLoS ONE 7:e35571

Rubin M, Berman-Frank I, Shaked Y (2011) Dust- and mineral-iron utilization by the marine dinitrogen-fixer *Trichodesmium*. Nat Geosci 4:529–534

Shi T, Sun Y, Falkowski PG (2007) Effects of iron limitation on the expression of metabolic genes in the marine cyanobacterium *Trichodesmium erythraeum* IMS101. Environ Microbiol 9:2945–2956

Shi D, Xu Y, Hopkinson BM, Morel FMM (2010) Effect of ocean acidification on iron availability to marine phytoplankton. Science 327:676–679

Shi D, Kranz SA, Kim J-M, Morel FMM (2012) Ocean acidification slows nitrogen fixation and growth in the dominant diazotroph *Trichodesmium* under low-iron conditions. Proc Natl Acad Sci USA 109:E3094

Shi D, Shen R, Kranz SA, Morel FMM, Hong H (2017) Response to Comment on "The complex effects of ocean acidification on the prominent N_2-fixing cyanobacterium *Trichodesmium*". Science 357:eaao0428

Snow JT et al (2015a) Environmental controls on the biogeography of diazotrophy and *Trichodesmium* in the Atlantic Ocean. Glob Biogeochem Cycle 29:865–884

Snow JT et al (2015b) Quantifying integrated proteomic responses to iron stress in the globally important marine diazotroph *Trichodesmium*. PLoS ONE 10:e0142626

Sobotka R (2014) Making proteins green; biosynthesis of chlorophyll-binding proteins in cyanobacteria. Photosynth Res 119:223–232

Sohm JA, Webb EA, Capone DG (2011) Emerging patterns of marine nitrogen fixation. Nat Rev Microbiol 9:499–508

Sreekumar PG, Hinton DR, Kannan R (2011) Methionine sulfoxide reductase A: structure, function and role in ocular pathology. World J Biol Chem 2:184–192

Sunda WG, Price NM, Morel FMM (2005) Trace metal ion buffers and their use in culture studies. In: Andersen RA (ed) Algal culturing techniques. Elsevier, Amsterdam, pp 35–63

Tandeau De Marsac N, Houmard J (1988) Complementary chromatic adaptation: physiological conditions and action spectra. In: Packer L, Glazer AN (eds) Methods in enzymology, vol 167. Cyanobacteria. Academic, San Diego, pp 318–328

Thornton LE, Ohkawa H, Roose JL, Kashino Y, Keren N, Pakrasi HB (2004) Homologs of plant PsbP and PsbQ proteins are necessary for regulation of photosystem ii activity in the cyanobacterium *Synechocystis* 6803. Plant Cell 16:2164–2175

Walworth NG et al (2016) Mechanisms of increased *Trichodesmium* fitness under iron and phosphorus co-limitation in the present and future ocean. Nat Commun 7:1–11

Wen L-S, Jiann K-T, Santschi PH (2006) Physiochemical speciation of bioactive trace metals (Cd, Cu, Fe, Ni) in the oligotrophic South China Sea. Mar Chem 101:104–129

Yousef N, Pistorius EK, Michel KP (2003) Comparative analysis of *idiA* and *isiA* transcription under iron starvation and oxidative stress in *Synechococcus elongatus* PCC 7942 wild-type and selected mutants. Arch Microbiol 180:471–483

Zappa S, Bauer CE (2017) The maintenance of iron homeostasis among prokaryotic phototrophs. In: Hallenbeck P (ed) Modern topics in the phototrophic prokaryotes. Springer, Cham, pp 123–161

Zhang H, Byrne RH (1996) Spectrophotometric pH measurements of surface seawater at in situ conditions: absorbance and protonation behavior of thymol blue. Mar Chem 52:17–25

Zouni A, Witt HT, Kern J, Fromme P, Krauss N, Saenger W, Orth P (2001) Crystal structure of photosystem II from *Synechococcus elongatus* at 3.8 A resolution. Nature 409:739–743